REGULAR ARTICLE

blood advances

# RUNX1 mutations enhance self-renewal and block granulocytic differentiation in human in vitro models and primary AMLs

Mylène Gerritsen,[1] Guoqiang Yi,[2] Esther Tijchon,[2] Jorren Kuster,[2] Jan Jacob Schuringa,[1] Joost H. A. Martens,[2] and Edo Vellenga[1]

[1]Department of Hematology, University Medical Centre Groningen, University of Groningen Cancer Research Centre, Groningen, The Netherlands; and [2]Department of Molecular Biology, Radboud Institute for Molecular Life Sciences, Nijmegen, The Netherlands.

**Key Points**

- RUNX1 mutations lead to a block in granulocytic differentiation that can be partially rescued by *CEBPA* overexpression.
- RUNX1 mutations deregulate gene expression on specific loci.

To unravel molecular mechanisms by which Runt-related transcription factor 1 (RUNX1) mutations contribute to leukemic transformation, we introduced the RUNX1-S291fs300X mutation in human $CD34^+$ stem/progenitor cells and in human induced pluripotent stem cells (iPSCs). In both models, RUNX1mut overexpression strongly impaired myeloid commitment. Instead, self-renewal was enhanced, as shown, by increased long-term culture-initiating cell frequencies and enhanced colony-forming cell replating capacity. Long-term suspension cultures with RUNX1mut-transduced cord blood (CB) $CD34^+$ cells continued for more than 100 days, during which the cells displayed an immature granulocyte-macrophage progenitor-like $CD34^+/CD123^+/CD45RA^+$ phenotype. The $CD34^+/CD38^-$ hematopoietic stem cell (HSC) population most likely acted as cell of origin, as HSCs provided the best long-term proliferative potential on overexpression of RUNX1mut. *CEBPA* expression was reduced in RUNX1mut cells, and reexpression of *CEBPA* partly restored differentiation. RNA-seq analysis on CB/iPSC systems and on primary patient samples confirmed that RUNX1 mutations induce a myeloid differentiation block, and that a common set of RUNX1mut-upregulated target genes was strongly enriched for gene ontology terms associated with nucleosome assembly and chromatin structure. Interestingly, in comparison with AML1-ETO binding in acute myeloid leukemias (AMLs), we found significantly distinct genomic distribution and differential expression for RUNX1mut of genes such as *TCF4*, *MEIS1*, and *HMGA2* that may potentially contribute to the underlying difference in clinical outcomes between RUNX1mut and AML1-ETO patients. In conclusion, RUNX1mut appears to induce a specific transcriptional program that contributes to leukemic transformation.

## Introduction

Aberrations in the functionality of transcription factor Runt-related transcription factor 1 (RUNX1) are linked to myeloid malignancies. Mutations in the RUNX1 gene (RUNX1mut) have been identified in myelodysplasia[1-4] and de novo and secondary acute myeloid leukemia (AML),[5] and are generally associated with unfavorable clinical outcomes.[6] Familial RUNX1 mutations are associated with familial thrombocytopenia, and patients have a predisposition to AML development.[7,8] In addition to the point mutations in the RUNX1 gene, a number of fusion partners of RUNX1 and their deregulating functions have been described in detail, including AML1-ETO,[9] whereas mutations in RUNX1 have hardly been studied.

RUNX1 is essential during multiple stages in the hematopoietic development, including the formation of definitive HSCs,[5,10] B-cell maturation,[11] megakaryocyte maturation, and granulocytic differentiation.[12] RUNX1

Submitted 6 August 2018; accepted 24 December 2018. DOI 10.1182/bloodadvances.2018024422.

The full-text version of this article contains a data supplement.

mutations, both heterozygous and homozygous, are located along the full length of the protein. This usually results in single amino-acid substitutions in the DNA-binding domain or in C-terminal truncation mutations lacking all or part of the activation domain.[13-16] Loss-of-function studies in mice have demonstrated that RUNX1 deficiency is associated with an expansion of the common myeloid progenitors and granulocyte-macrophage progenitor (GMP) pool, which could be rescued by inactivation of *Hmga2*.[17] In addition, RUNX1 loss leads to an increased susceptibility to AML development in collaboration with MLL-ENL and *N*-Ras, suggesting that RUNX1 has a tumor-suppressor function.[18,19] However, recent work has illustrated the importance of RUNX1wt expression in AML1-ETO and MLL-AF9 cells, suggesting a prosurvival function in leukemogenesis.[20]

Here, we studied the in vitro growth and the RUNX1 binding pattern and expression profile induced by the C-terminal-truncating RUNX1-S291fs300X mutant in cord blood (CB) $CD34^+$ cells and induced pluripotent stem cells (iPSCs). We then compared these findings with those from primary RUNX1mut AMLs. The results indicate that a single RUNX1 mutation leads to increased self-renewal, enhanced long-term culture-initiating cell (LTC-IC) frequency, and long-term maintenance of $CD34^+$ cells. Chromatin immunoprecipitation (ChIP)-seq and RNA-seq experiments, including primary AML samples, indicate that RUNX1 mutations, independent of the model, induce a unique transcriptional program. By comparing the effects of RUNX1mut with the programs triggered by AML1-ETO, we found that RUNX1mut targets several other genes that possibly affect the clinical outcomes of these 2 types of leukemia.

## Materials and methods

### Human cells

Umbilical CB was derived after healthy full-term pregnancies from the obstetrics departments of the Martini Hospital and the University Medical Centre in Groningen, The Netherlands. Normal bone marrow cells were derived from healthy volunteers or extracted from healthy hipbone after hip replacement surgery, after informed consent. Peripheral blood stem cells were extracted after stem cell mobilization from patients, after informed consent. AML blasts from peripheral blood or bone marrow from patients with de novo AML were studied after informed consent was obtained, in accordance with the Declaration of Helsinki. The protocol was approved by the Ethical Review Board of the University Medical Center Groningen, Groningen, The Netherlands. To obtain relative pure cell populations and the largest fraction of leukemic cells, fluorescence-activated cell sorting (FACS) based on expression of cell surface marker CD33 or CD34 was performed. An overview of all mutations can be found in supplemental Table 2, and more information about these AMLs is described in Yi et al.[21] The megakaryoblast-derived iPSCs were obtained from Sanquin Amsterdam.[22] Full culture methods and differentiation of RUNX1mut iPSCs toward the granulocytic lineage are described in the supplemental Methods.

### Flow cytometry

Surface marker analysis was performed on the LSR-II (BD Biosciences). A list of antibodies can be found in the supplemental Methods.

### Immunoblotting

Whole-cell extracts were prepared by boiling an appropriate number of cells in Laemmli sample buffer for 5 minutes with subsequent separation on 10% sodium dodecyl sulfate-acrylamide gels. Proteins were transferred to PVDF (Millipore), using wet transfer. RUNX1 was detected with α-RUNX1 antibody (Abcam 23980) 1:2000 and β-actin (Abcam 16039).

### CEBPA rescue experiments

Weeks 8 to 10, CB RUNX1mut cells were transduced with retroviral vector containing CEPBA fused to the estrogen receptor domain (described previously[23]). Transduced cells were sorted and plated in growth medium with and without 100 nM 4-hydroxytamoxifen. After 3 days, expression of cell surface markers and RNA expression was determined.

### RNA extraction and cDNA synthesis

RNA was extracted from $1 \times 10^6$ iPSC control and RUNX1mut cells, using the RNeasy mini kit (Qiagen), including on-column DNaseI treatment. Ribosomal RNA was depleted by using the ribo-zero rRNA removal kit (Illumina). RNA was fragmented in 300-bp fragments by incubation for 7.5 minutes in fragmentation buffer (200 mM Tris-acetate, 500 mM potassium acetate, 150 mM magnesium acetate at pH 8.2). First-strand cDNA synthesis was performed using superscript III (Life Technologies), followed by synthesis of the second cDNA strand.

### Chromatin immunoprecipitation

Cells were crosslinked with 1% formaldehyde for 10 minutes at room temperature at a concentration of $15 \times 10^6$ cells/mL. The fixed cells were sonicated for 5 minutes (30 seconds on, 30 seconds off), using the Diagenode Bioruptor. Sonicated chromatin was centrifuged for 10 minutes at maximum speed and then incubated with either 5 μg RUNX1 antibody (Abcam ab23980) that recognizes both RUNX1wt and RUNX1mut proteins or 2 μg flag M2 antibody that recognizes the overexpressed RUNX1mut protein (Sigma F3165). Beads were washed with 4 different wash buffers, and chromatin was eluted from the beads. DNA proteins were de-crosslinked, and samples were purified using the Qiaquick MinElute PCR purification kit. Library preparation, Illumina high-throughput sequencing, and ChIP-seq and RNA-seq data analysis is described in detail in the supplemental Materials.

### Statistical analysis

A paired or unpaired 2-sided Student *t* test was used to calculate statistical differences. $P < .05$ was considered statistically significant. Error bars represent standard deviation: $^*P < .05$; $^{**}P < .01$; $^{***}P < .001$.

## Results

### RUNX1mut cells display impaired erythroid differentiation, but increased myeloid replating capacity and expansion

CB $CD34^+$ cells were transduced with the RUNX1 mutant S291fs300X (RUNX1mut; Figure 1A), and overexpression was confirmed by quantitative reverse transcription polymerase chain

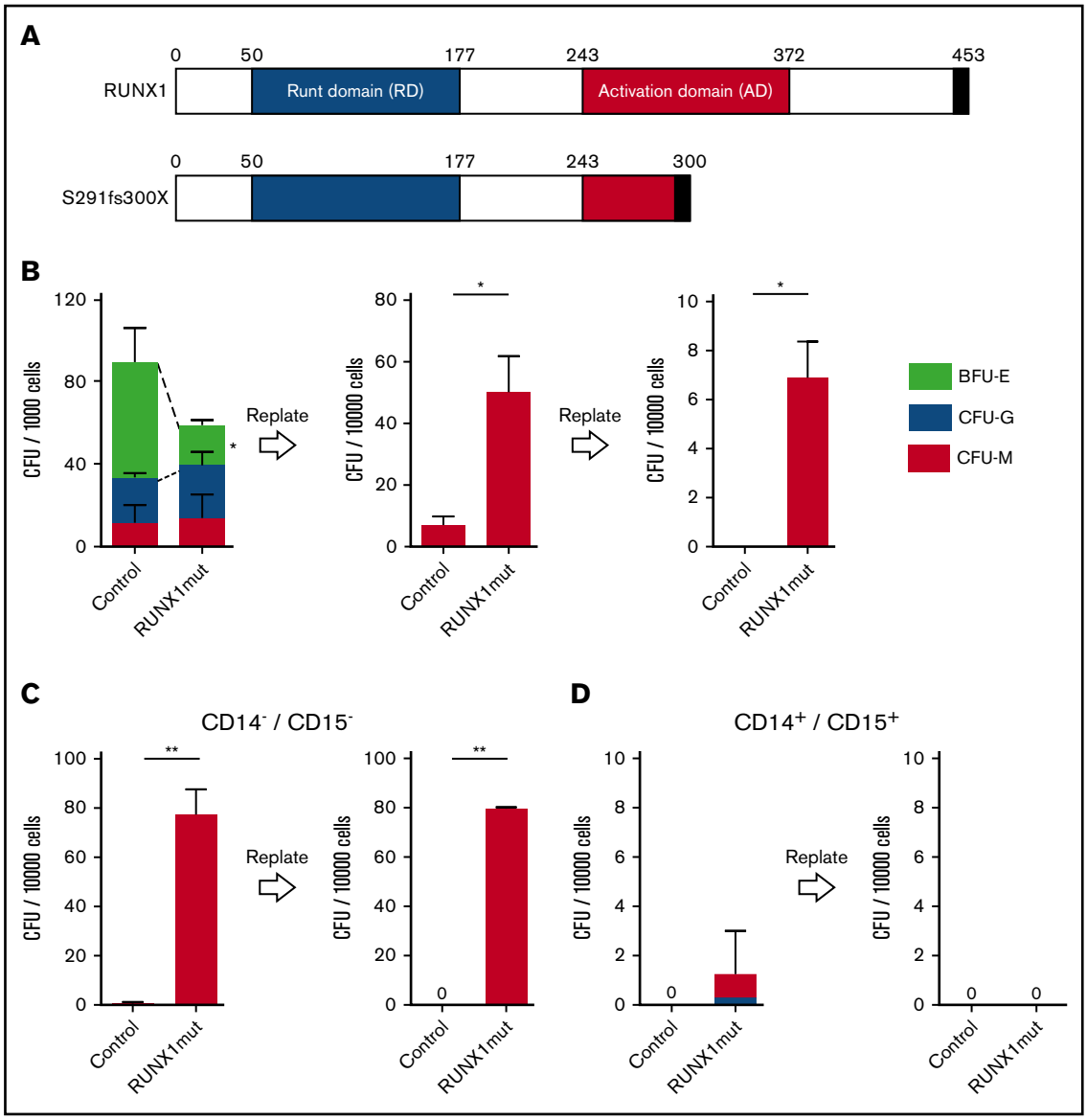


**Figure 1. RUNX1mut increases replating capacity.** (A) Schematic overview of RUNX1wt and RUNX1 S291fs300X mutant. (B) CFC and replating potential of RUNX1mut vs control. At the start, 500 cells were plated per dish in duplicates. Between days 10 to 14, the number of colonies were scored and all colonies were harvested. For each replating, 25 000 cells per dish were plated. Replating potential of control vs RUNX1mut in the $CD14^-/CD15^-$ fraction (C) and replating potential of control vs RUNX1mut in the $CD14^+/CD15^+$ fraction (D). At the start, 500 cells were plated per dish in duplicates. Between days 10 and 14, the number of colonies were scored and colonies were harvested and stained for CD14 and CD15. In a new CFC, 25 000 $CD14^+$ or $CD15^+$ cells and 25 000 $CD14^-/CD15^-$ cells were FACS sorted. After 10 to 14 days, this was repeated for another replating round. *$P < .05$; **$P < .01$.

reaction (qRT-PCR; supplemental Figure 1A). The progenitor frequency was determined by colony-forming cell (CFC) assay. A decline in erythroid burst-forming unit (BFU-E) formation was observed without a difference in CFU-G or CFU-M colony formation (Figure 1B). In addition to a reduction in BFU-E numbers, the colony morphology reflected an immature appearance (data not shown), which was linked to a reduced expression of *GATA1*, an important regulator of erythroid differentiation (supplemental Figure 1B). In addition, a strong reduction in expansion was observed when CB $CD34^+$ RUNX1mut cells were cultured under erythroid-permissive conditions (supplemental Figure 1C). In contrast, the CFC replating capacity of myeloid progenitors was enhanced on overexpression of RUNX1mut (Figure 1B). This was especially the case in the more primitive $CD14^-/CD15^-$ cell fraction compared with the more differentiated $CD14^+/CD15^+$ fraction (Figure 1C-D).

To determine whether RUNX1mut-transduced cells could also be propagated for a longer period in the context of a bone marrow microenvironment, CB $CD34^+$ RUNX1mut cells were cultured on MS5 bone marrow stroma (Figure 2A; supplemental Figure 2A). No significant growth advantage was observed for the RUNX1mut cells compared with control CB $CD34^+$ cells. However, RUNX1mut-transduced cells were maintained under the stroma, without significant expansion, for up to 10 to

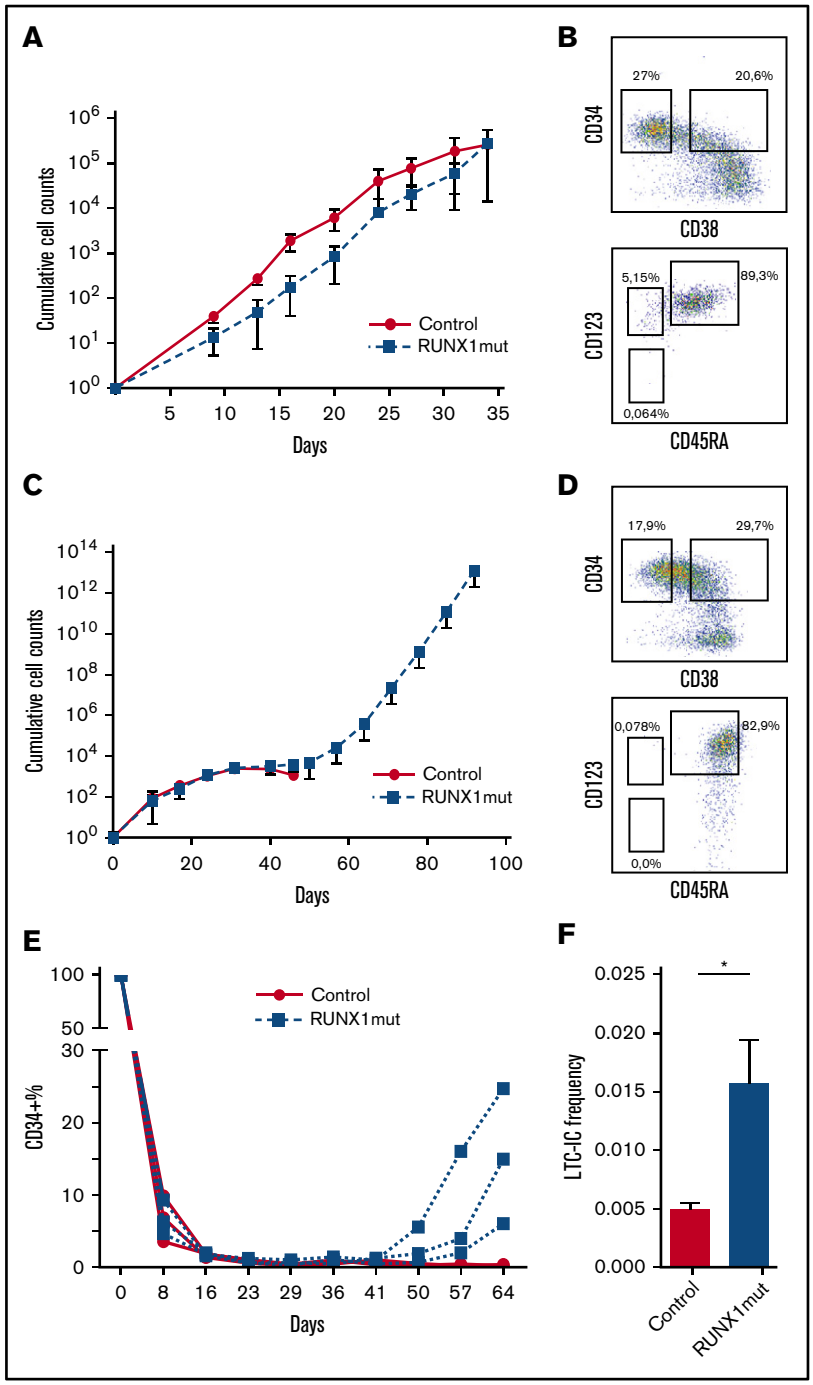


**Figure 2. RUNX1mut-transduced CB CD34$^+$ cells have increased growth potential, LTC-IC-frequency, and CD34$^+$ maintenance.** (A) Relative expansion in MS5 coculture of control vs RUNX1mut. Growth curve of MS5 coculture (5 weeks). After 5 weeks, the MS5 was replated (see supplemental Figure 2A for continued growth). (B) Marker expression analysis of adherent fraction of RUNX1mut cells in MS5 coculture after 10 weeks. Expansion of suspension fraction was very limited and did not allow for surface marker expression after 10 weeks. (C) Relative expansion in liquid culture over a course of several weeks in control vs RUNX1mut (n = 3). (D) Marker expression analysis of RUNX1mut cells in liquid culture after 10 weeks. (E) CD34$^+$ expression of 3 CB control vs RUNX1mut cells in time. Each line represents a different culture. (F) LTC-IC frequency of control vs RUNX1mut cells. *$P < .05$.

12 weeks. FACS analysis of these stroma-adherent RUNX1mut cells after 10 weeks of culture revealed that a high proportion of the cells, in contrast to the control cells (supplemental Figure 2B), had a persistent immature phenotype, as shown by expression of CD34$^+$/CD38$^-$ and high expression of CD123 and CD45RA (Figure 2B).

In addition, long-term myeloid suspension cultures were initiated to study the growth potential of CB CD34$^+$ RUNX1mut cells during a longer period without a bone marrow microenvironment (Figure 2C). Control transduced cells fully differentiated to macrophages after 8 weeks of culture, whereas the RUNX1mut CB cell culture had a persistent population of more immature monoblastic cells that expanded for more than 3 months (supplemental Figure 2C). Further characterization of RUNX1mut cells by FACS analysis at week 10 identified a mixture of CD34$^+$ and CD34$^-$ cells (Figure 2D). CD34$^-$ cells were CD14$^+$/CD15$^-$ (supplemental Figure 2D), whereas the CD34$^+$ cell population consisted of a CD38$^+$ and a large CD38$^-$ subfraction, suggesting a HSC phenotype. The CD34$^+$ CD38$^+$ fraction strongly expressed both CD123 and CD45RA,

suggesting an accumulation at the GMP stage (Figure 2D). In addition to these phenotypic markers, at week 10, RUNX1mut cells also showed increased expression of several markers that have been described on leukemic stem cells, such as CD116, IL1RAP, and CD135 (supplemental Figure 2E).[24] We observed an initial loss of the $CD34^+$, which reappeared after 6 to 7 weeks of culture (Figure 2E). Based on the observed differentiation block and the high percentage of $CD38^-$ in our MS5 coculture, we hypothesized that RUNX1mut had induced distinct phenotypes in the immature stem cell fraction ($CD34^+CD38^-$) relative to the mature ($CD34^+/CD38^+$) progenitor cell fraction. To test this hypothesis, CB cells were transduced with RUNX1mut and sorted for $CD34^+CD38^-$ and $CD34^+CD38^+$ cells, and then expanded in suspension cultures over time (supplemental Figure 2F). The immature cell population with blast cell morphology originated mostly in the $CD34^+/CD38^-$ fraction, whereas the $CD34^+/CD38^+$ fraction had a higher amount of fully differentiated macrophages (supplemental Figure 2G), suggesting that the HSC population acts as the cell of origin. This is in line with the findings of an increased stem cell frequency of CB $CD34^+$ RUNX1mut cells after 4 weeks of stromal cocultures (Figure 2F). To exclude the possibility that the long-term expansion was limited to fetal-CB-derived $CD34^+$ cells, adult bone marrow (n = 2, not shown) and adult peripheral blood (n = 2) $CD34^+$ cells were transduced with the RUNX1mut construct (supplemental Figure 2H). In all the experiments, long-term expansion for 10 weeks was obtained and provided a similar phenotype. These findings indicate that expression of the RUNX1mut impairs myeloid and erythroid maturation, results in a differentiation block at the GMP stage, and enhances CFC replating and stem cell frequencies.

## The RUNX1mut phenotype is characterized by low CEBPA expression and can be partially rescued by re-expression of CEBPA

We hypothesized that the differentiation block could be abolished by culturing RUNX1mut cells in granulocytic differentiation medium containing granulocyte colony-stimulating factor (G-CSF). Interestingly, G-CSF did not induce granulocytic differentiation, in contrast to control cells (supplemental Figure 3A). FACS analyses showed that the RUNX1mut cells lost the expression of the G-CSF receptor (CD114) over time (Figure 3A). We therefore analyzed the expression levels of several known RUNX1 target genes important for granulocytic differentiation, such as *CEBPA* and *SPI1*. This analysis showed a 2-fold decline in *CEBPA* expression, a key regulator of granulocytic differentiation (Figure 3B). With the publicly available TCGA data set, we identified 16 AMLs with a RUNX1 mutation and confirmed that a reduced expression of *CEBPA* is a common feature of RUNX1mut-expressing cells, in comparison with RUNX1wt (supplemental Table 1; Figure 3C).[25] To determine whether *CEBPA* downregulation was the main cause of the observed GMP differentiation block, we overexpressed a CEBPA-ER fusion construct in week 10 RUNX1mut $CD34^+$ cells. Stimulation with 4OH-tamoxifen resulted in a decline in expansion, increased expression of CD15 and CD14, and decreased expression of CD34 (Figure 3D). Morphological studies revealed a rapid decline in monoblastic-like cells after 3 days of culture (Figure 3E), but no granulocytic cells were observed. qRT-PCR and FACS revealed only a limited increase of *CD114* mRNA levels and cell surface expression (supplemental Figure 1A; supplemental Figure 3C), whereas *CTSG* and *MPO*, 2 important genes involved in granulocytic differentiation, were not altered, suggesting that *CEBPA* is an important downstream target of RUNX1mut, but also that other targets might be crucial in this deregulated granulocytic differentiation.

## RUNX1mut expression in differentiating iPSC model results in a differentiation block of the myeloid lineage by direct regulation of RUNX1mut target genes

As a second method to model the effect of the RUNX1mut without interference from additional mutations, we used iPSCs. In these cells, expression of the RUNX1mut was induced during hematopoietic development in vitro (Figure 4A). The tetracycline-inducible promoter enables effective RUNX1mut expression because of the addition of doxycycline (supplemental Figure 4A-B). Expression of the RUNX1mut was induced directly after mesoderm differentiation (day 0) or at various stages during hematopoietic development (days 6, 10, 14). Phenotyping the cells over time revealed a retained expression of CD34 on RUNX1mut expression (Figure 4B; supplemental Figure 4C) and a decreased number of differentiated ($CD15^+$) cells in RUNX1mut-expressing cells compared with non-induced cells (Figure 4C). Induction of RUNX1mut at early times (day 0) resulted in a short delaying effect on HSC formation, but otherwise no abnormal differentiation was observed. In combination with the monoblastic appearance of these cells (supplemental Figure 4D), this suggests a block in differentiation, similar to that observed for the CB data. These data were corroborated by RNA-seq analysis of control vs dox-induced iPSCs, which revealed, similar as for the CB model, reduced levels of *CEBPA* in the RUNX1mut-expressing cells (Figure 4D).

## Identification of a RUNX1mut-specific gene program

To determine the relevance of the RUNX1 target genes in primary AML cells, we then compared transcriptional differences initiated by RUNX1mut by RNA-seq in CB-RUNX1mut cells, iPSC-RUNX1mut cells, normal bone marrow $CD34^+$ (GSE63569),[26] monocytes, macrophages, and granulocytes, as well as to patient AML cells harboring RUNX1mut (supplemental Figure 5A). PCA analysis based on expression revealed clustering of specific cell types and $CD34^+$ cells: most of the undifferentiated cell populations, including the iPSC and CB models, clustered on 1 side of the PCA, and the differentiated cells on the opposite side (Figure 5A). To map the compositional difference of RUNX1mut-expressing cells systematically, we used the CIBERSORT deconvolution method.[27] This showed that a large proportion of the cell population was carrying not only a $CD34^+$ progenitor signature but also a substantial monocytic signature, whereas a granulocytic signature was nearly absent (Figure 5B). We also found that genes normally expressed in granulocytes showed decreased expression levels in RUNX1mut-expressing models and primary AMLs, whereas the expression levels of monocytic-related genes were comparable (Figure 5C; supplemental Figure 5B-C). This indicates that RUNX1mut cells maintain a progenitor phenotype featured by monocytic characteristics, but only granulocytic genes were dramatically repressed by aberrant RUNX1 protein, suggesting that RUNX1mut predominantly affects granulocytic differentiation.

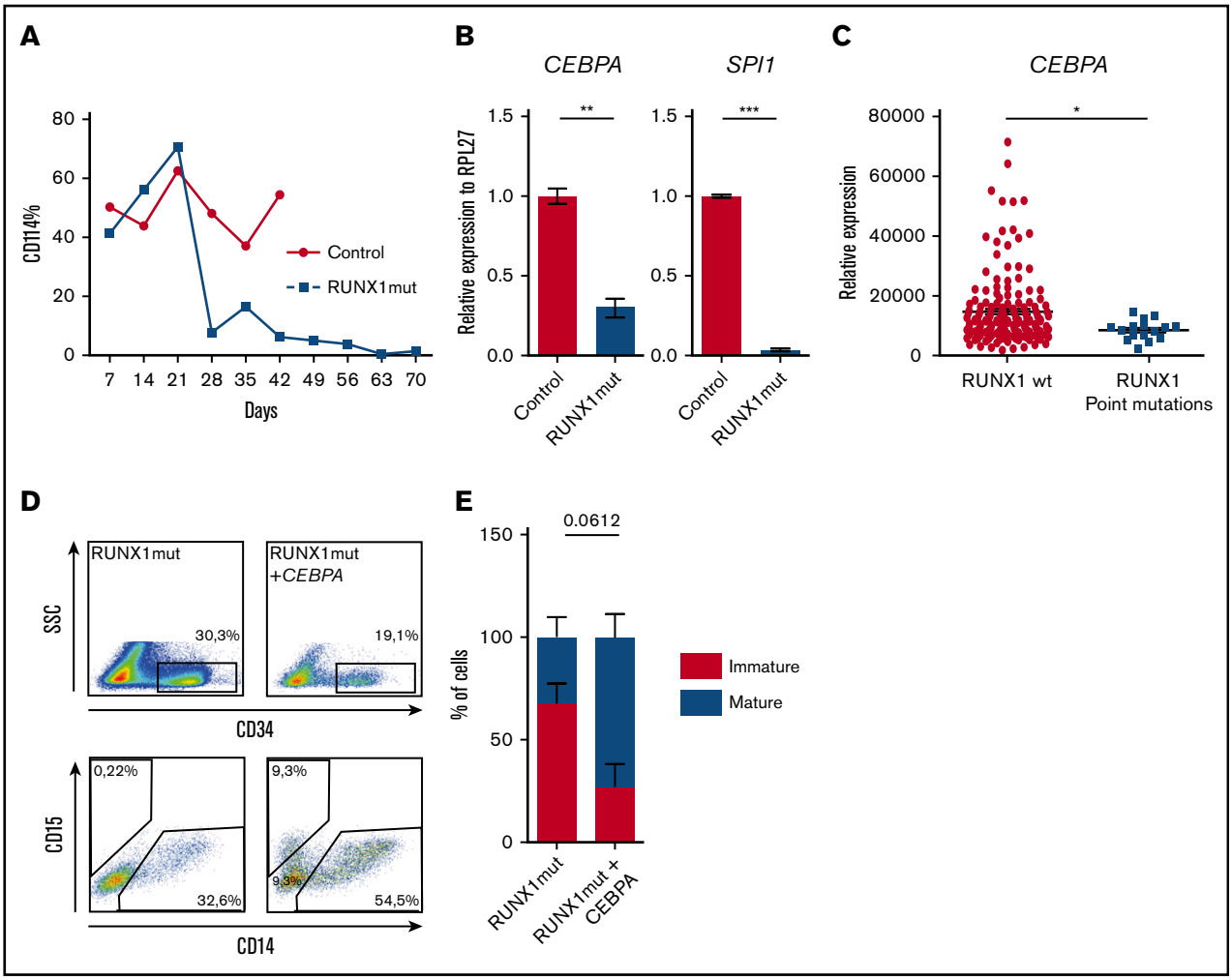


**Figure 3. CEBPA expression is decreased in RUNX1mut cells.** (A) CD114 expression of CB control vs RUNX1mut cells in time in cells cultured with G-CSF. (B) qRT-PCR analysis of *CEBPA*, an *SPI1* expression in control vs RUNX1mut after ~2 weeks of expansion in liquid culture medium. (C) Relative *CEBPA* expression in RUNX1wt vs RUNX1mut AMLs in the TCGA data set. AML1-ETO or inv(16) AMLs are excluded from this analysis. (D) Immature marker (CD34) and immature markers (CD14 and CD15) expression before and after 3 days of overexpression of CEBPA-ER induced by tamoxifen. (E) Percentage of mature and immature-appearing cells in RUNX1mut and RUNX1mut + CEBPA cells after 3 days of overexpression of CEBPA. Two hundred cells were score a rated mature or immature on the basis of their morphology. $^{*}P < .05$; $^{**}P < .01$; $^{***}P < .001$.

Using k-means clustering, we visualized differentially expressed genes between RUNX1mut-expressing cells and normal CD34$^{+}$ HSPCs (Figure 5D). This revealed 4 clusters, of which cluster 4 represents 556 genes that are downregulated in all RUNX1mut-expressing groups compared with normal CD34$^{+}$ cells. This cluster comprises enrichment for genes involved in inflammation and immune response, suggesting an effect on myeloid cell maturation (Figure 5E). Cluster 3 represents a set of 542 genes commonly upregulated in all RUNX1mut-expressing cells, but not in CD34$^{+}$ cells. This RUNX1mut-specific gene cluster is enriched for genes related to chromatin organization, including several small nucleolar RNAs, thus suggesting a role in RNA processing.

This transcriptome-wide exploration indicates that in vitro RUNX1mut models can recapitulate the altered transcriptional landscape induced by RUNX1mut in patient AML cells. Moreover, it identified the RUNX1mut-specific program in the primary AMLs, suggesting that the additional transcriptional alterations in these AML cells (eg, in cluster 1 and 2) might be a result of other genetic lesions.

## Global RUNX1mut binding in CB and iPSC models binding in primary AMLs with RUNX1 mutations

To define binding sites of RUNX1 and compare these within our CB and iPSC models and primary AMLs, we performed ChIP and ChIP-seq analysis, using an antibody recognizing both RUNX1wt and RUNX1mut (Figure 6A; supplemental Figure 6A). This revealed binding of RUNX1 in RUNX1mut-transduced CB cells (CB-RUNX1mut) and in RUNX1mut-expressing iPSC (iPSC-RUNX1mut) at similar sites as those in primary RUNX1mut AMLs (Figure 6A). We found similar RUNX1 occupancy profiles in control iPSCs, although with lower density (Figure 6A-B). We identified 895 high-confidence RUNX1 binding sites shared among CB-RUNX1mut, iPSC-RUNX1mut, and primary AMLs with a RUNX1 mutation (supplemental Figure 6B). Functional analysis of the genes

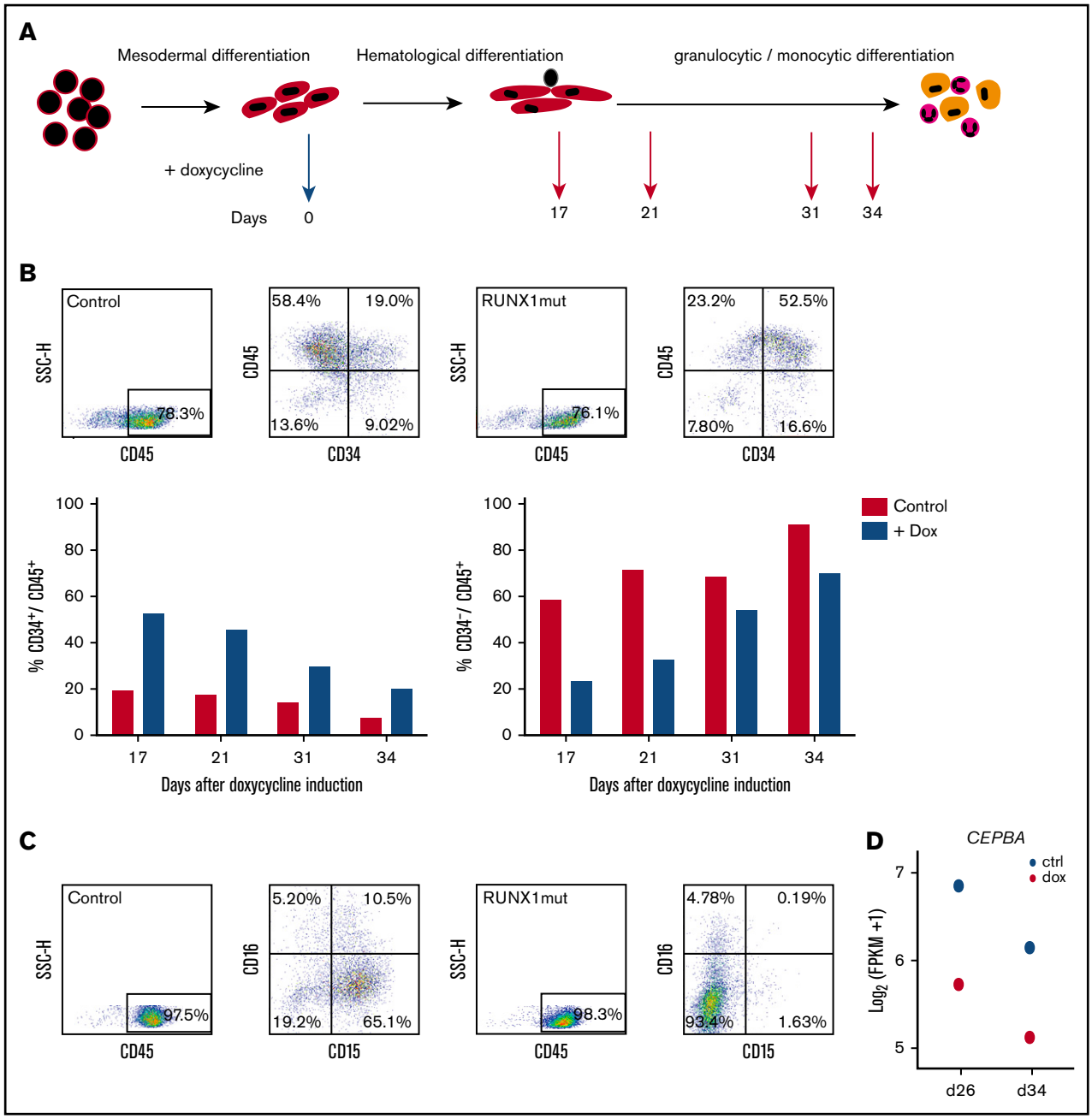


**Figure 4. iPSC differentiation is impaired when expressing RUNX1mut.** (A) Time schedule of iPSC differentiation protocol and marker expression analysis. At the beginning of the hematological differentiation (blue arrow), doxycycline is added, inducing expression of RUNX1mut. Cell surface marker expression on CD34/CD45 was performed on different points (red arrows). (B) Example of marker analysis and a representable figure of $CD34^+/CD45^+$ and $CD34^-/CD45^+$ expression on different points during differentiation. (C) Marker analysis and a representable figure of CD15 and CD16 expression in control vs RUNX1mut-expressing iPSCs on day 17 of differentiation. (D) Log2 expression levels of *CEBPA* in control vs dox-induced iPS cells.

associated with overlapping RUNX1 binding sites revealed enrichment for processes associated with transcription and translation (supplemental Figure 6C).

As RUNX1 binding has been associated with regulating the local epigenetic environment, we investigated the epigenetic state of the common RUNX1 binding sites by examining epigenetic data of RUNX1mut AMLs.[21] In line with the observation that most of the common RUNX1mut binding sites are in promoters or near genes (supplemental Figure 6D-E), our analysis revealed enrichment for active chromatin marks such as DNaseI accessibility, H3K4me3 and H3K27ac (supplemental Figure 6F), and association of RUNX1 binding with genes that are actively transcribed (supplemental Figure 6G). This is in accordance with the reduced levels of repressive marks such as H3K27me3.

To determine whether this state is different in RUNX1wt AML cells, we then compared the epigenetic state at RUNX1 binding sites

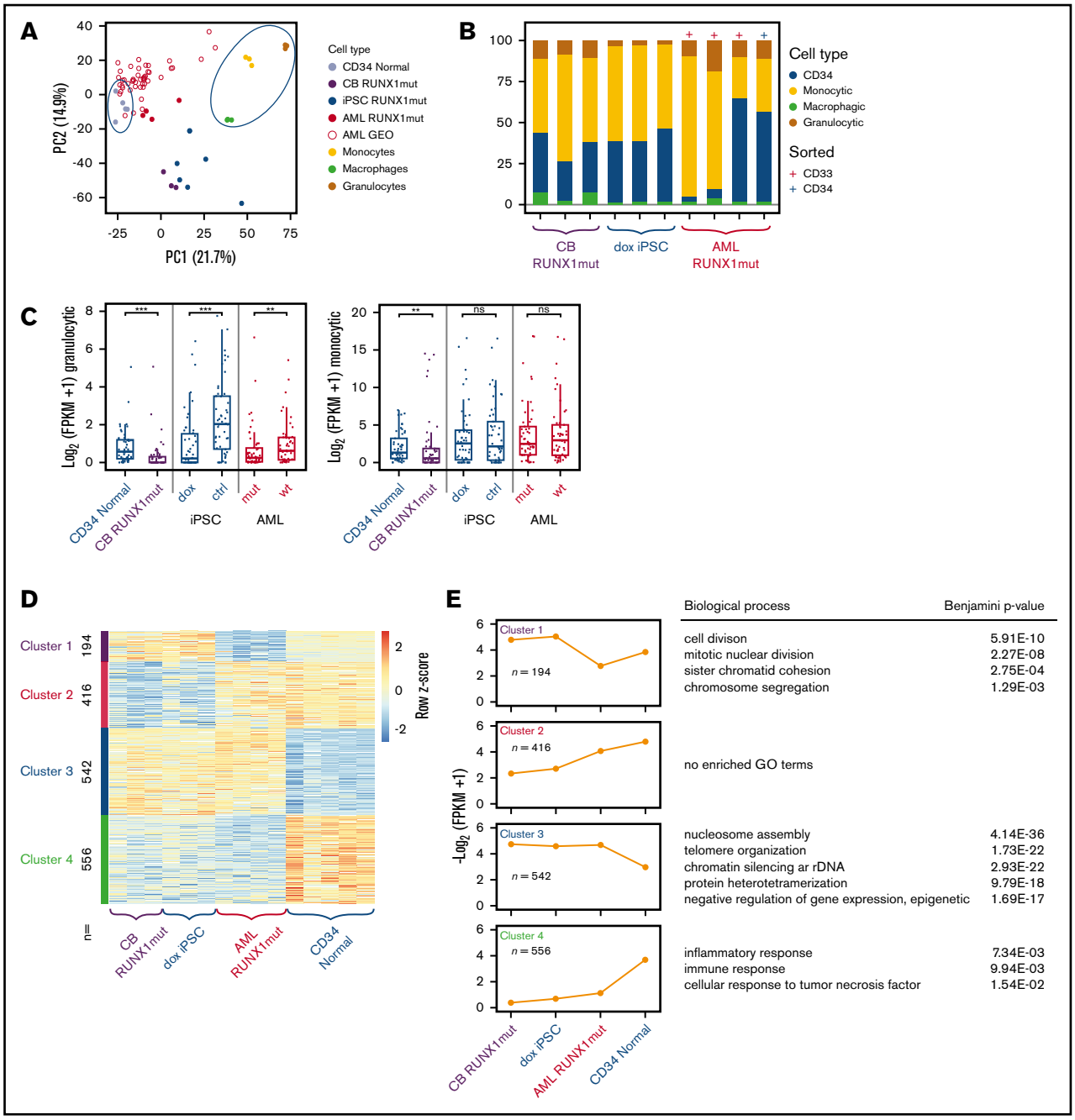


**Figure 5. The RUNX1mut gene program.** (A) PCA plot using RNA-seq results of the indicated cell types. Hollow circle indicates RNA-seq data from published primary AMLs carrying RUNX1mut (https://leucegene.ca/research-development/). Normal cells are indicated within the blue circles. (B) Based on RNA-seq predicted average fraction of $CD34^+$ cells, granulocytes, monocytes, and macrophages in RUNX1mut-expressing cells, using CIBERSORT. (C) Differential expression of monocytic and granulocytic signature genes in normal CD34 cells, RUNX1mut expressing CB cells, iPSC models, and primary AML cells. (D) Heat map of gene expression by k-means clustering in RUNX1mut-expressing CB, iPSC, and primary AML cells vs control $CD34^+$ cells resulting in 4 main clusters. (E) Biological process enrichment for each of the 4 clusters identified in panel D. $^{**}P < .01$; $^{***}P < .001$. ns, not significant.

common in RUNX1wt and RUNX1mut AMLs and the transcriptional state of their target genes (supplemental Figure 6H). This showed no global differences between RUNX1wt and RUNX1mut AMLs in the presence of active or repressive marks at the common RUNX1 binding sites (supplemental Figure 6I), suggesting the absence of a common epigenetic deregulating mechanism by RUNX1mut. Interestingly, target gene expression still varied significantly between RUNX1wt and RUNX1mut AMLs, with approximately half the target genes upregulated and half the target genes downregulated in RUNX1mut AML cells (Figure 6C, middle). These alterations in gene activity at the local level did correlate with epigenetic alterations, as exemplified for *NUCB2*

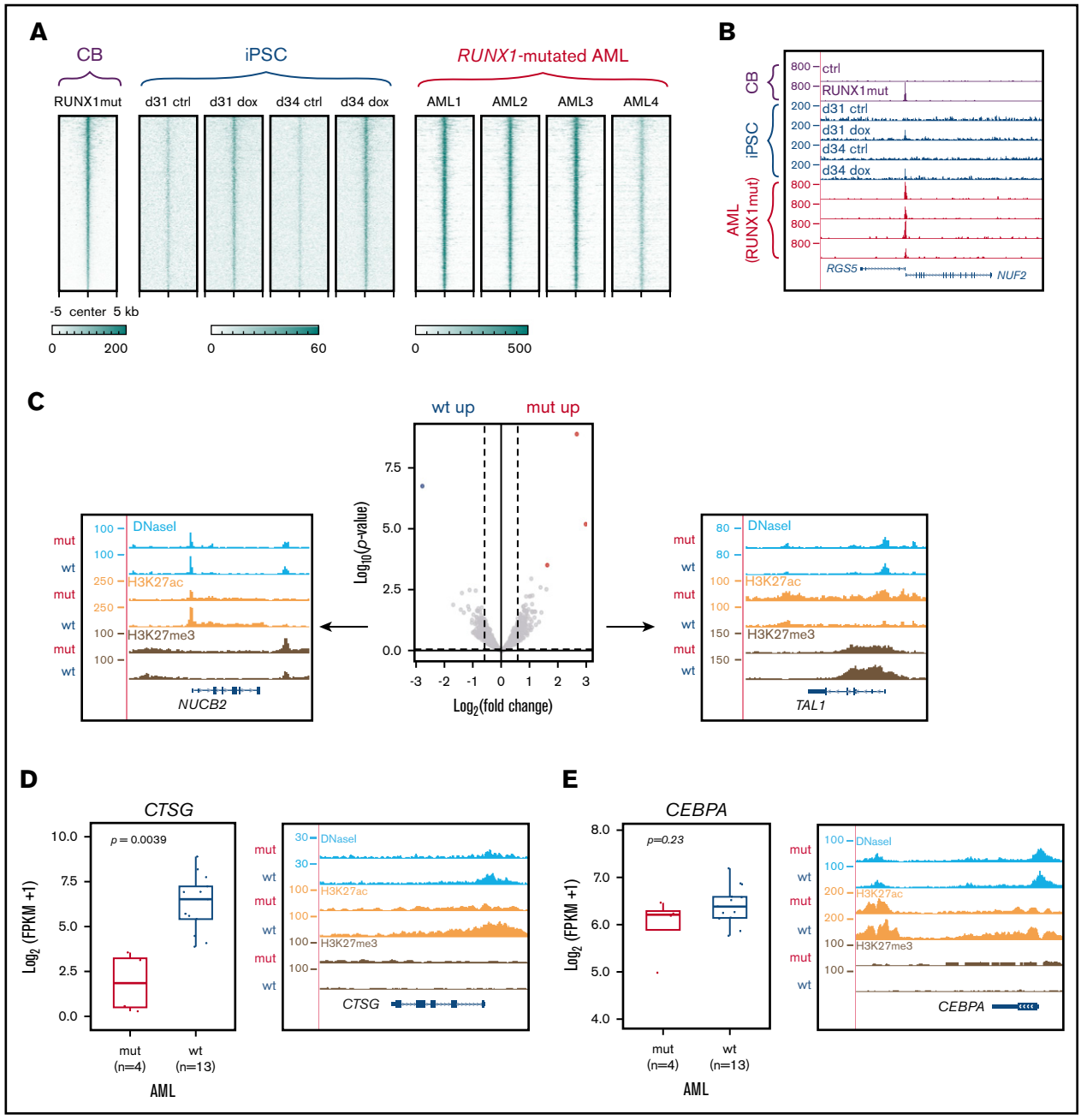


**Figure 6. RUNX1 binding in model cells and primary AMLs.** (A) Heat map of RUNX1mut-binding sites in RUNX1mut-transduced CB cells, control and RUNX1mut-induced iPSCs, and primary AMLs with RUNX1mut. (B) Screenshot of RUNX1 binding in CB-RUNX1mut and control cells, iPSC-RUNX1mut cells with and without dox, and primary AMLs expressing RUNX1mut. (C) Differential expression of genes that are bound by RUNX1 in both RUNX1wt and RUNX1mut AMLs. NUCB2 (left) is higher expressed in RUNX1wt AMLs, whereas TAL1 (right) is expressed more in RUNX1mut AMLs. Differential levels of H3K27ac are associated with the levels of expression. (D) Expression levels and levels of DNaseI, H3K27ac, and H3K27me3 at the *CTSG* locus in RUNX1wt vs RUNX1mut AMLs. (E) Expression levels and levels of DNaseI, H3K27ac, and H3K27me3 at the *CEBPA* locus in RUNX1wt vs RUNX1mut AMLs.

(up in RUNX1wt) and *TAL1* (up in RUNX1mut; Figure 6C, left and right).

For a more general view, we zoomed into the genes that have differential expression on RUNX1mut expression (Figure 5D, clusters 3 and 4), and found that the levels of active chromatin marks (mainly H3K27ac and H3K4me3) were higher in genes that are upregulated compared with the genes that are downregulated (supplemental Figure 6J). Levels of H3K27me3 were low overall, and were not altered. For example, for *CTSG*, we found decreased expression coinciding with less H3K27ac (Figure 6D), whereas this was not observed for genes that are not differentially expressed (supplemental Figure 6K). Expression of *CEBPA* was also decreased, but not significantly, possibly because of a limited number of studied AMLs. However, we did see a

decrease in H3K27ac (Figure 6E), supporting our cell biological data.

These results suggest that RUNX1mut does not have a global effect on the epigenetic state at its binding sites, but has specific effects on genes important for granulocytic and monocytic differentiation.

### RUNX1mut and AML1-ETO have different target genes

In view of the difference in clinical outcome between RUNX1mut AMLs and AML-ETO AMLs, we investigated the difference in oncogene binding. We identified 12 792 RUNX1mut and 4170 AML1-ETO peaks in our primary AMLs and found partial overlap for RUNX1mut and AML1-ETO (supplemental Figure 7A). Subsequently, we included recently published data on AML1-EVI1 binding.[28] When comparing peak distributions from these data sets, we found that RUNX1mut peaks are mostly located in promoters, whereas AML1-ETO and AML1-EVI1 are intergenic, suggesting distinct occupancy and regulatory roles resulting from the 3 types of mutations (Figure 7A). Also, analysis of the genes in the direct vicinity (+5 kb, −1 kb; Figure 7B) identified only a small number of direct AML1-ETO and AML1-EVI1 target genes. In this study, we showed that in our iPSC model, RUNX1mut, similar as shown for AML1-ETO (E.T., G.Y., Amit Mandoli, Jos G. A. Smits, Francesco Ferrari, Falco Wijnen, Bowon Kim, Eva M. Janssen-Megens, J.J.S., and J.H.A.M., manuscript in preparation; Mandoli et al[29]; supplemental Figure 7B), is involved in repressing granulocytic differentiation. However, when comparing specific gene expression changes, we observed that key granulocytic genes such as *MPO* and *CTSG* are more deregulated in the RUNX1mut-expressing cells (Figure 7C; supplemental Figure 7C). Upregulated genes in RUNX1mut iPSCs, but not in AML1-ETO iPSCs, include *MEIS1*, *TCF4*, *ERG*, and *HMGA2*, genes previously described as being upregulated in leukemogenesis (supplemental Figure 7C; supplemental Table 3). Interestingly, comparing RUNX1 binding differences in RUNX1mut and AML1-ETO primary AMLs showed decreased binding of RUNX1 at many of these genes, including *TCF4*, *HMGA2*, and *MN1,* in AML1-ETO AMLs (Figure 7D). In addition, we found that RUNX1mut AMLs have decreased expression of granulocytic genes such as *CEBPE* and *ELANE* (Figure 7E; supplemental Table 4). Upregulated genes in RUNX1mut AMLs include genes important for signal transduction and hematopoiesis, again including *TCF4*, *MN1*, and *MEIS1* (Figure 7E-F).

Finally, we were interested in whether we could rescue the overexpression of these genes by CEBPA re-expression, as we had conducted in our CB models. These results show that *MEIS1*, *HMGA2*, and *CD34* were downregulated on overexpression of CEBPA (supplemental Figure 7D), suggesting that CEBPA-mediated differentiation might result in a decreased stem cell phenotype.

In conclusion, our results suggest that RUNX1mut occupies and regulates different loci compared with AML1-ETO, and triggers different gene expression patterns at a number of critical genes relevant for granulocytic differentiation.

## Discussion

To unravel the mechanisms by which RUNX1 mutations contribute to leukemic transformation, we investigated the cell biological and molecular consequences of a RUNX1 mutation as single genetic hit in healthy CB-derived $CD34^+$ cells and in human iPSCs. The resulting data were compared with those from RUNX1-mutated and wild-type primary AML patient cells, and from patient samples expressing the AML1-ETO fusion protein, which display rather different molecular and clinical characteristics. This comparison showed that the RUNX1 truncation mutant S291fs300X induces a differentiation block when introduced into CB $CD34^+$ cells or iPSCs. This results in the emergence of GMP-like cells, which also express IL1-RAP, with increased self-renewal potential in vitro.

The differentiation block at the GMP stage is linked to a reduced expression of *CEBPA* in the myeloid lineage, which has been described as a main deregulated gene in AML1-ETO.[30] In our study, re-expression of *CEBPA* partially rescued the differentiation block, which is also in line with findings in AML1-ETO AMLs.[31] RNA-seq analysis showed transcriptional differences regarding the presence of the RUNX1mut in human in vitro models and primary AMLs when compared with normal bone marrow $CD34^+$ cells, thereby identifying several clusters. PCA analysis of our RNA-seq data revealed an enrichment of stem cell genes and a loss of genes for granulocytic differentiation, reflecting the differentiation block induced by the RUNX1mut. This suggests that RUNX1mut dictates a distinct transcriptional program in favor of transformation.

We analyzed model systems that have only 1 RUNX1 mutation, thus excluding all secondary effects caused by additional mutations, and identified genes directly deregulated by RUNX1mut. Our approach therefore has little overlap with a recent study that compared RUNX1mut AMLs with RUNX1wt AMLs.[32] This is in line with the findings that RUNX1mut requires additional mutations frequently found together with RUNX1mut, including *ASXL1*[33] or elevated *BMI1* expression,[2] that epigenetically influence the expression of another set of target genes.

By using ChIP-seq, we linked RUNX1mut binding to differences in histone modifications, revealing that RUNX1mut did not completely reshape the localization of epigenetic marks. The analysis showed that RUNX1mut can both induce and repress target genes, and that this is associated with the amount of activating histone modifications, mainly H3K27ac, suggesting a more gene-specific regulation of transcription. This differs from the activity of AML1-ETO, which has been shown to bind mainly to introns and intergenic regions that are enriched in accessible chromatin, marked with p300, but are generally low in acetylation.[34] Also, on direct gene binding, AML1-ETO leads to gene repression, and thus has a dominant negative effect relative to native AML1 by recruiting HDACs, NCoR, and mSin3A.[35-38]

Transcriptional differences between RUNX1mut and AML1-ETO in our iPSC models and primary AML cells include *HMGA2*,[17] *TCF4*,[39] and *MEIS1*.[40] Previous studies have shown that the expression of these genes is increased in AMLs, which makes them potentially important targets of RUNX1mut, but not for AML1-ETO in leukemogenesis.

In summary, the results of cellular assays, transcriptomic and epigenomic profiling of human CB and iPSC models expressing RUNX1 mutations,

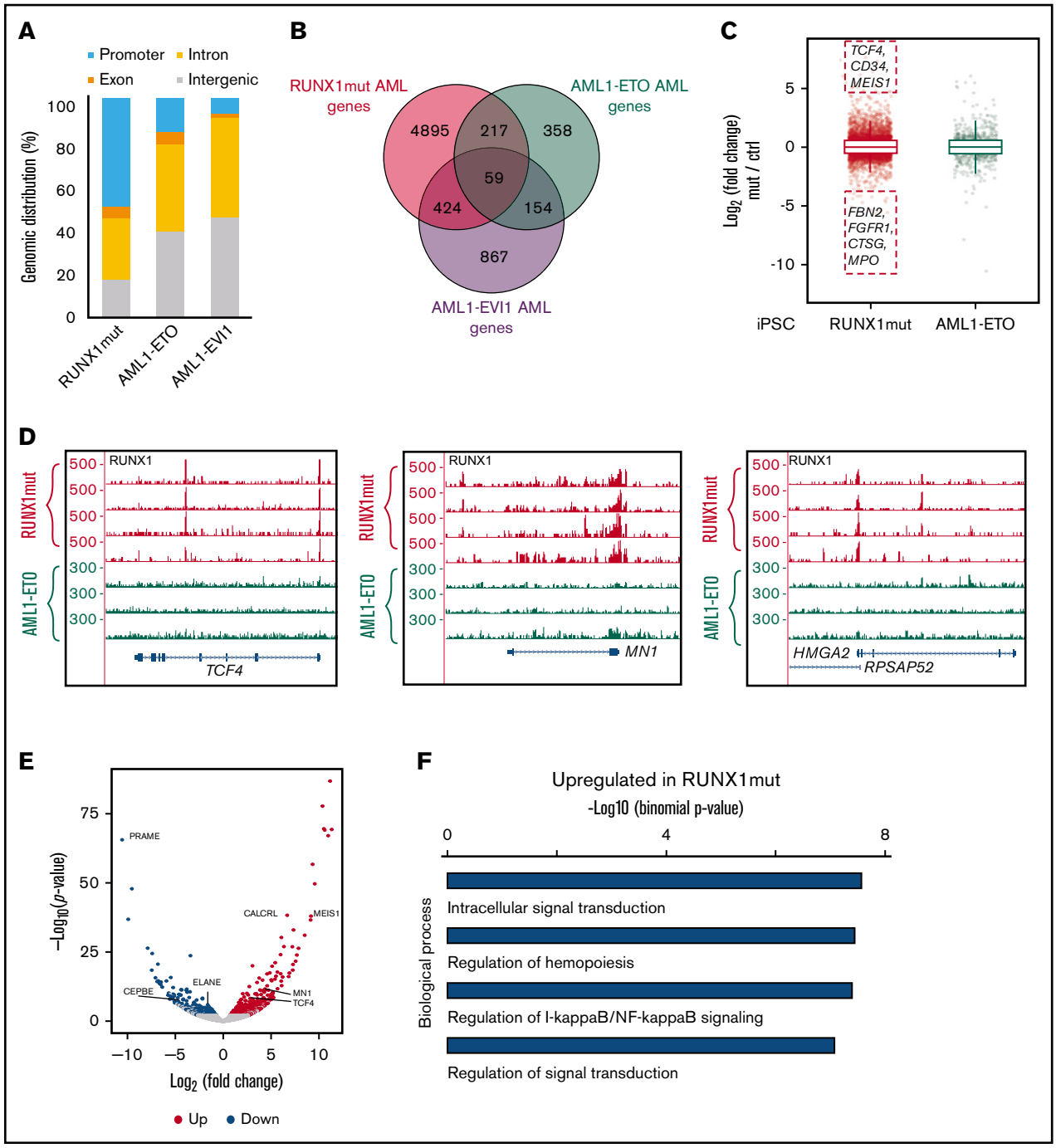


**Figure 7. RUNX1mut vs AML1-ETO.** (A) Genomic distribution of RUNX1mut, AML1-ETO, and AML1-EVI1 binding sites. All peaks are assigned to promoters (2 kb away from TSS), exons, introns, and intergenic regions based on the physical distance. The priority rule of category assignment: promoter > exon > intron > intergenic region. (B) Gene overlap of RUNX1mut, AML1-ETO, and AML1-EVI1 binding sites selected by +5 kb, −1 kb distance. (C) Differential expression of RUNX1mut and AML1-ETO iPSC. Several significant genes regulated by RUNX1 or AML1-ETO are highlighted. (D) Differential binding of RUNX1 in RUNX1mut and AML1-ETO primary AML samples. (E) Differential expression between 4 RUNX1mut AMLs and 3 AML1-ETO AMLs. (F) Biological processes enriched for genes upregulated in RUNX1mut AMLs compared with AML1-ETO AMLs.

demonstrate that RUNX1 binding and RNA expression recapitulate the effects of RUNX1-mutated primary AMLs. This indicates a change in the RUNX1-dependent cellular programming that is independent of additional mutations. This programming differs between RUNX1mut and AML1-ETO-positive AMLs. This could potentially explain the different clinical outcomes of patients with AML harboring an RUNX1 mutation (poor risk) and those harboring an AML1-ETO (good risk) translocation.

## Acknowledgments

The authors thank Jenny Jaques and Fiona van der Heuvel for their technical assistance.

## Authorship

Contribution: M.G., G.Y., E.T., J.J.S., J.H.A.M., and E.V. conceived and planned the experiments; M.G., G.Y., E.T., and J.K. carried out the experiments; M.G., G.Y., E.T., J.K., J.J.S., J.H.A.M., and E.V. contributed to the interpretation of the results; M.G. took the lead in writing the manuscript; and all authors provided critical feedback and helped shape the research, analysis and manuscript.

Conflict-of-interest disclosure: The authors declare no competing financial interests.

ORCID profiles: M.G., 0000-0002-1464-9535; J.J.S., 0000-0001-8452-8555.

Correspondence: Edo Vellenga, University Medical Center Groningen, Department of Hematology, Hanzeplein 1, 9713 GZ Groningen, The Netherlands; e-mail: e.vellenga@umcg.nl.

## References

1. Harada Y, Harada H. Molecular pathways mediating MDS/AML with focus on AML1/RUNX1 point mutations. *J Cell Physiol*. 2009;220(1):16-20.
2. Harada Y, Inoue D, Ding Y, et al. RUNX1/AML1 mutant collaborates with BMI1 overexpression in the development of human and murine myelodysplastic syndromes. *Blood*. 2013;121(17):3434-3446.
3. Haferlach T, Nagata Y, Grossmann V, et al. Landscape of genetic lesions in 944 patients with myelodysplastic syndromes. *Leukemia*. 2014; 28(2):241-247.
4. Bejar R, Stevenson K, Abdel-Wahab O, et al. Clinical effect of point mutations in myelodysplastic syndromes. *N Engl J Med*. 2011; 364(26):2496-2506.
5. Ichikawa M, Yoshimi A, Nakagawa M, Nishimoto N, Watanabe-Okochi N, Kurokawa M. A role for RUNX1 in hematopoiesis and myeloid leukemia. *Int J Hematol*. 2013;97(6):726-734.
6. Haferlach T, Stengel A, Eckstein S, et al. The new provisional WHO entity 'RUNX1 mutated AML' shows specific genetics but no prognostic influence of dysplasia. *Leukemia*. 2016;30(10):2109-2112.
7. Song WJ, Sullivan MG, Legare RD, et al. Haploinsufficiency of CBFA2 causes familial thrombocytopenia with propensity to develop acute myelogenous leukaemia. *Nat Genet*. 1999;23(2):166-175.
8. Liew E, Owen C. Familial myelodysplastic syndromes: a review of the literature. *Haematologica*. 2011;96(10):1536-1542.
9. Gaidzik VI, Bullinger L, Schlenk RF, et al. RUNX1 mutations in acute myeloid leukemia: results from a comprehensive genetic and clinical analysis from the AML study group. *J Clin Oncol*. 2011;29(10):1364-1372.
10. Tober J, Yzaguirre AD, Piwarzyk E, Speck NA. Distinct temporal requirements for Runx1 in hematopoietic progenitors and stem cells. *Development*. 2013;140(18):3765-3776.
11. Dowdy CR, Frederick D, Zaidi SK, et al. A germline point mutation in Runx1 uncouples its role in definitive hematopoiesis from differentiation. *Exp Hematol*. 2013;41(11):980-991.
12. Guo H, Ma O, Speck NA, Friedman AD. Runx1 deletion or dominant inhibition reduces Cebpa transcription via conserved promoter and distal enhancer sites to favor monopoiesis over granulopoiesis. *Blood*. 2012;119(19):4408-4418.
13. Osato M, Asou N, Abdalla E, et al. Biallelic and heterozygous point mutations in the runt domain of the AML1/PEBP2alphaB gene associated with myeloblastic leukemias. *Blood*. 1999;93(6):1817-1824.
14. Osato M. Point mutations in the RUNX1/AML1 gene: another actor in RUNX leukemia. *Oncogene*. 2004;23(24):4284-4296.
15. Preudhomme C, Warot-Loze D, Roumier C, et al. High incidence of biallelic point mutations in the Runt domain of the AML1/PEBP2 alpha B gene in Mo acute myeloid leukemia and in myeloid malignancies with acquired trisomy 21. *Blood*. 2000;96(8):2862-2869.
16. Tang JL, Hou HA, Chen CY, et al. AML1/RUNX1 mutations in 470 adult patients with de novo acute myeloid leukemia: prognostic implication and interaction with other gene alterations. *Blood*. 2009;114(26):5352-5361.
17. Lam K, Muselman A, Du R, et al. Hmga2 is a direct target gene of RUNX1 and regulates expansion of myeloid progenitors in mice. *Blood*. 2014; 124(14):2203-2212.
18. Nishimoto N, Arai S, Ichikawa M, et al. Loss of AML1/Runx1 accelerates the development of MLL-ENL leukemia through down-regulation of p19ARF. *Blood*. 2011;118(9):2541-2550.
19. Motoda L, Osato M, Yamashita N, et al. *Runx1* protects hematopoietic stem/progenitor cells from oncogenic insult. *Stem Cells*. 2007; 25(12):2976-2986.
20. Goyama S, Schibler J, Cunningham L, et al. Transcription factor RUNX1 promotes survival of acute myeloid leukemia cells. *J Clin Invest*. 2013; 123(9):3876-3888.
21. Yi G, Wierenga ATJ, Petraglia F, et al. Chromatin-based classification of genetically heterogeneous AMLs into two distinct subtypes with diverse stemness phenotypes. *Cell Reports*. 2019;26(4):1059-1069.
22. Hansen M, Varga E, Wüst T, et al. Generation and characterization of human iPSC line MML-6838-Cl2 from mobilized peripheral blood derived megakaryoblasts. *Stem Cell Res (Amst)*. 2017;18:26-28.

23. Wierenga ATJ, Schepers H, Moore MAS, Vellenga E, Schuringa JJ. STAT5-induced self-renewal and impaired myelopoiesis of human hematopoietic stem/progenitor cells involves down-modulation of C/EBPalpha. *Blood*. 2006;107(11):4326-4333.

24. Bonardi F, Fusetti F, Deelen P, van Gosliga D, Vellenga E, Schuringa JJ. A proteomics and transcriptomics approach to identify leukemic stem cell (LSC) markers. *Mol Cell Proteomics*. 2013;12(3):626-637.

25. Ley TJ, Miller C, Ding L, et al; Cancer Genome Atlas Research Network. Genomic and epigenomic landscapes of adult de novo acute myeloid leukemia. *N Engl J Med*. 2013;368(22):2059-2074.

26. Dolatshad H, Pellagatti A, Fernandez-Mercado M, et al. Disruption of SF3B1 results in deregulated expression and splicing of key genes and pathways in myelodysplastic syndrome hematopoietic stem and progenitor cells [published correction appears in *Leukemia*. 2015;29(8):1798]. *Leukemia*. 2015; 29(5):1092-1103.

27. Newman AM, Liu CL, Green MR, et al. Robust enumeration of cell subsets from tissue expression profiles. *Nat Methods*. 2015;12(5):453-457.

28. Loke J, Assi SA, Imperato MR, et al. RUNX1-ETO and RUNX1-EVI1 differentially reprogram the chromatin landscape in t(8;21) and t(3;21) AML. *Cell Reports*. 2017;19(8):1654-1668.

29. Mandoli A, Singh AA, Prange KHM, et al. The hematopoietic transcription factors RUNX1 and ERG prevent AML1-ETO oncogene overexpression and onset of the apoptosis program in t(8;21) AMLs. *Cell Reports*. 2016;17(8):2087-2100.

30. Pabst T, Mueller BU, Harakawa N, et al. AML1-ETO downregulates the granulocytic differentiation factor C/EBPalpha in t(8;21) myeloid leukemia. *Nat Med*. 2001;7(4):444-451.

31. Loke J, Chin PS, Keane P, et al. C/EBPα overrides epigenetic reprogramming by oncogenic transcription factors in acute myeloid leukemia. *Blood Adv*. 2018;2(3):271-284.

32. Simon L, Lavallée VP, Bordeleau ME, et al. Chemogenomic landscape of RUNX1-mutated AML reveals importance of RUNX1 allele dosage in genetics and glucocorticoid sensitivity. *Clin Cancer Res*. 2017;23(22):6969-6981.

33. Nagase R, Inoue D, Pastore A, et al. Expression of mutant Asxl1 perturbs hematopoiesis and promotes susceptibility to leukemic transformation. *J Exp Med*. 2018;215(6):1729-1747.

34. Saeed S, Logie C, Francoijs KJ, et al. Chromatin accessibility, p300, and histone acetylation define PML-RARα and AML1-ETO binding sites in acute myeloid leukemia. *Blood*. 2012;120(15):3058-3068.

35. Gelmetti V, Zhang J, Fanelli M, Minucci S, Pelicci PG, Lazar MA. Aberrant recruitment of the nuclear receptor corepressor-histone deacetylase complex by the acute myeloid leukemia fusion partner ETO. *Mol Cell Biol*. 1998;18(12):7185-7191.

36. Wang J, Hoshino T, Redner RL, Kajigaya S, Liu JM. ETO, fusion partner in t(8;21) acute myeloid leukemia, represses transcription by interaction with the human N-CoR/mSin3/HDAC1 complex. *Proc Natl Acad Sci USA*. 1998;95(18):10860-10865.

37. Lutterbach B, Westendorf JJ, Linggi B, et al. ETO, a target of t(8;21) in acute leukemia, interacts with the N-CoR and mSin3 corepressors. *Mol Cell Biol*. 1998;18(12):7176-7184.

38. Hildebrand D, Tiefenbach J, Heinzel T, Grez M, Maurer AB. Multiple regions of ETO cooperate in transcriptional repression. *J Biol Chem*. 2001; 276(13):9889-9895.

39. in 't Hout FEM, van der Reijden BA, Monteferrario D, Jansen JH, Huls G. High expression of transcription factor 4 (TCF4) is an independent adverse prognostic factor in acute myeloid leukemia that could guide treatment decisions. *Haematologica*. 2014;99(12):e257-e259.

40. Liu J, Qin YZ, Yang S, et al. Meis1 is critical to the maintenance of human acute myeloid leukemia cells independent of MLL rearrangements. *Ann Hematol*. 2017;96(4):567-574.